

内容

- 能带中的态密度
- 载流子的热平衡状态
- 热平衡状态下，半导体中载流子的分布概率
- 本征半导体中载流子浓度、费米能级的计算
- 杂质半导体中载流子浓度、费米能级的计算
- 简并半导体
- 非平衡载流子

上节内容回顾

$$g_c(E) = 4\pi V \left(\frac{2m_n^*}{h^2}\right)^{3/2} [E(k) - Ec]^{1/2}$$

$$g_v(E) = 4\pi V \left(\frac{2m_{dp}^*}{h^2}\right)^{3/2} [E_v - E(k)]^{1/2}$$

(态密度)

Fermi分布函数-电子占据能量E的几率

$$f(E) = \frac{1}{e^{\frac{E-E_F}{k_B T}} + 1}$$

电子的Boltzmann分布

$$\approx e^{\frac{E_F - E}{k_B T}} = f_B(E)$$

空穴占据的几率

$$1 - f(E) = \frac{1}{e^{\frac{-E+E_F}{k_B T}} + 1}$$

空穴的Boltzmann分布

$$\approx e^{\frac{E - E_F}{k_B T}}$$

导带的电子浓度 n_0

$$n_0 = \int_{E_C}^{E_{Top}} f(E) g_c(E) dE \approx \int_{Ec}^{\infty} f_B(E) g_c(E) dE$$

$$= N_c e^{(E_F - E_c)/k_B T}, \quad N_c = 2 \left[\frac{2\pi m_n^* k_B T}{h^2} \right]^{3/2}$$

—— 导带底的有效状态密度

价带顶的空穴浓度 p_0

$$p_0 = \int_{E_{Bottom}}^{E_V} g_V(E) [1 - f(E)] dE \approx \int_{-\infty}^{E_V} g_V(E) f_B(E) dE$$

$$= N_v e^{(E_V - E_F)/k_B T}, \quad N_v = 2 \left[\frac{2\pi m_p^* k_B T}{h^2} \right]^{3/2}$$

—— 价带顶的有效状态密度

$$n_0 = N_c e^{(E_F - E_c)/k_B T}$$

$$p_0 = N_v e^{(E_V - E_F)/k_B T}$$

$$n_0 = p_0 = n_i = (N_c N_v)^{1/2} e^{-\frac{E_g}{2k_B T}}$$

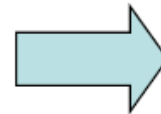
$$E_i = E_F = \frac{E_C + E_V}{2} + \frac{3k_0 T}{4} \ln \frac{m_p^*}{m_n^*}$$

本征半导体

浓度积 $n_o p_o$ 及影响因素

$$\begin{aligned} n_0 p_0 &= N_c N_v e^{-\frac{E_C - E_F}{k_B T}} e^{-\frac{E_F - E_V}{k_B T}} = N_c N_v e^{-\frac{E_g}{k_B T}} \\ &= 6.30 \times 10^{38} \left(\frac{m_n^* m_p^*}{m_0^2} \right)^{\frac{3}{2}} \left(\frac{T}{300K} \right)^3 e^{-\frac{E_g}{k_B T}} \text{ cm}^{-3} \end{aligned}$$

n_i 是材料和温度的函数，与 Fermi 能级无关（适合所有不掺杂与掺杂的情况）。即：在热平衡的条件下，所有半导体（本征半导体和掺杂半导体）都服从质量作用定律。



$$\therefore n_o p_0 = n_i^2$$

质量作用定律

n掺杂半导体中的载流子浓度和费米能级

1. 低温电离区

$$E_F = \frac{E_C + E_D}{2} + \frac{k_B T}{2} \ln \left[\frac{N_D}{2N_C} \right]$$

$$n_0 = \left[\frac{N_C N_D}{2} \right]^{1/2} e^{-\frac{\Delta E_D}{2k_B T}}$$

2. 饱和区

$$E_F = E_C + k_B T \ln \left[\frac{N_D}{N_C} \right]$$

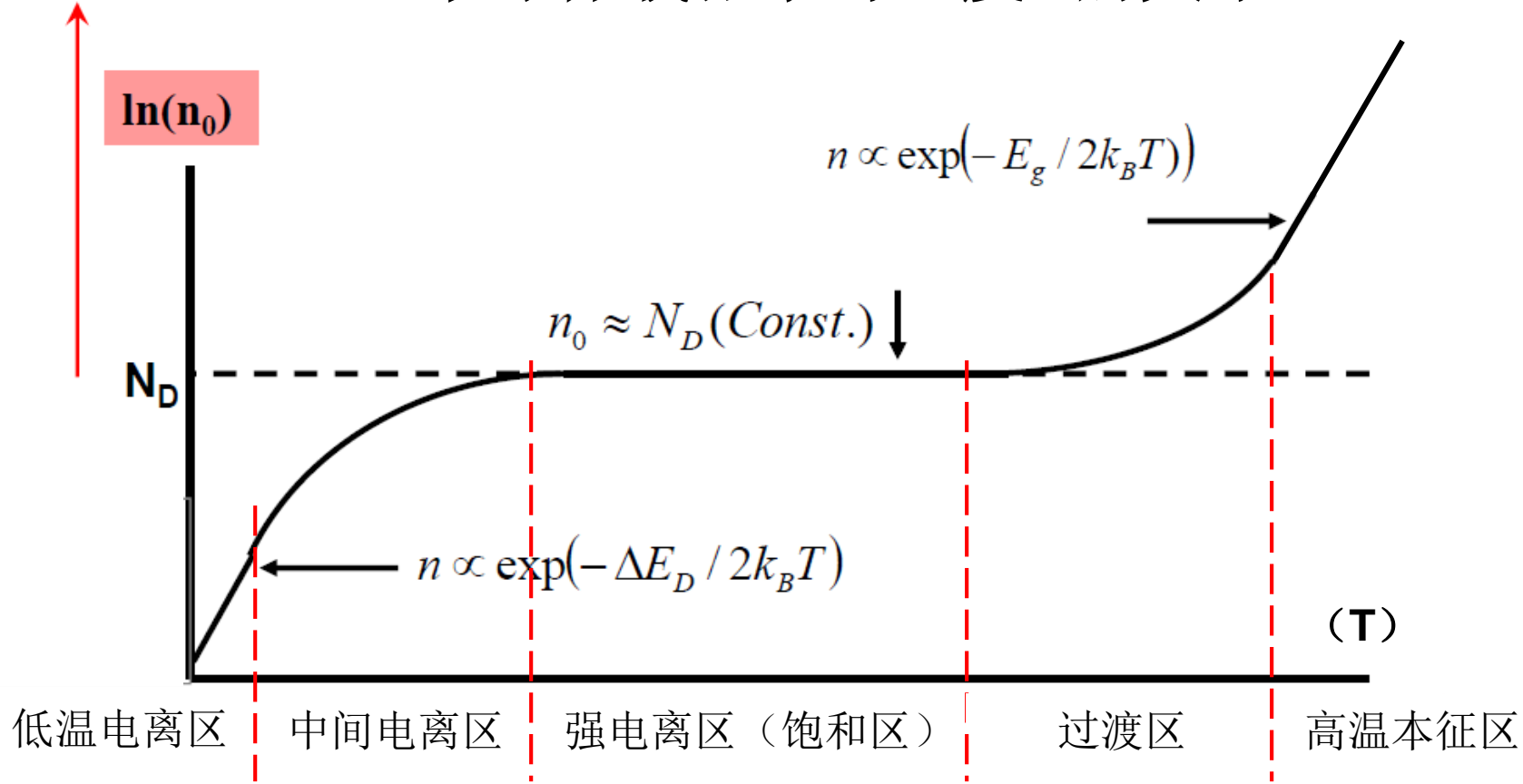
$$n_0 = n^+ = N_D$$

3. 高温本征区

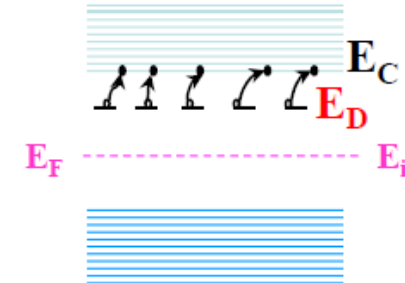
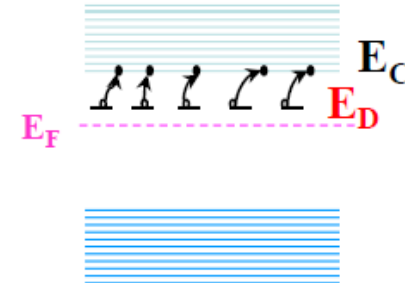
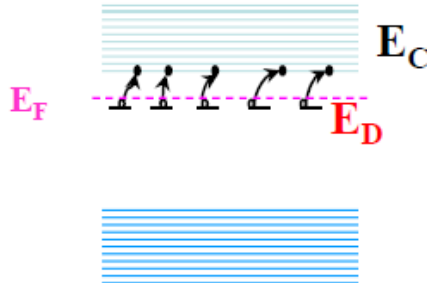
$$E_i = E_F = \frac{E_C + E_V}{2} + \frac{3k_0 T}{4} \ln \frac{m_p^*}{m_n^*}$$

$$n_i = (N_C N_V)^{1/2} e^{-\frac{E_g}{2k_B T}}$$

n型半导体载流子与温度T的关系



对应的
费米能级



p掺杂半导体中的载流子浓度和费米能级

P型半导体 $N_D = 0$

电中性条件

$$p_0 = n_0 + p_A^-$$

温度

$$E_f = \frac{E_A + E_V}{2} + \frac{kT}{2} \ln\left(\frac{2N_V}{N_A}\right)$$
$$p_0 = \left(\frac{N_A N_V}{2}\right)^{1/2} \exp\left(\frac{E_V - E_A}{2kT}\right)$$

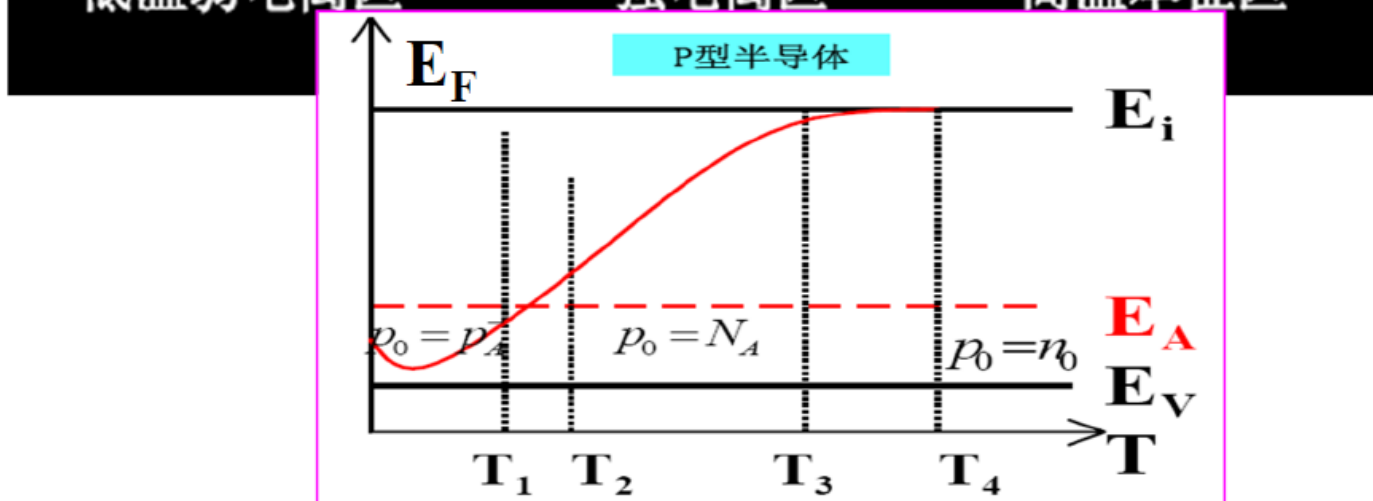
$$E_f = E_V + kT \ln\left(\frac{N_V}{N_A}\right)$$
$$p_0 = N_A$$

$$E_f = \frac{E_C + E_V}{2} + \frac{1}{2} \ln\left(\frac{N_V}{N_C}\right)$$
$$p_0 = n_0 = n_i$$

低温弱电离区

强电离区

高温本征区



少数载流子

◆ 少数载流子的求法：

(1) 通过多子浓度
(Hall measurement)

(2) 质量作用定理
($np=n_i^2$)

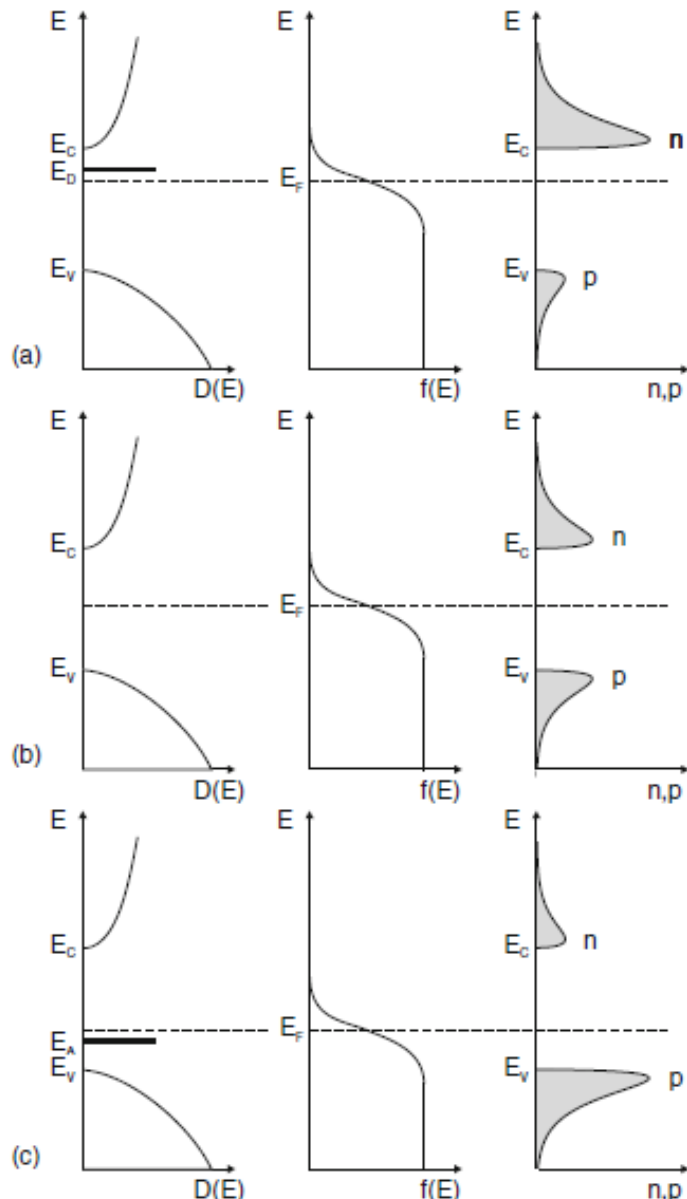
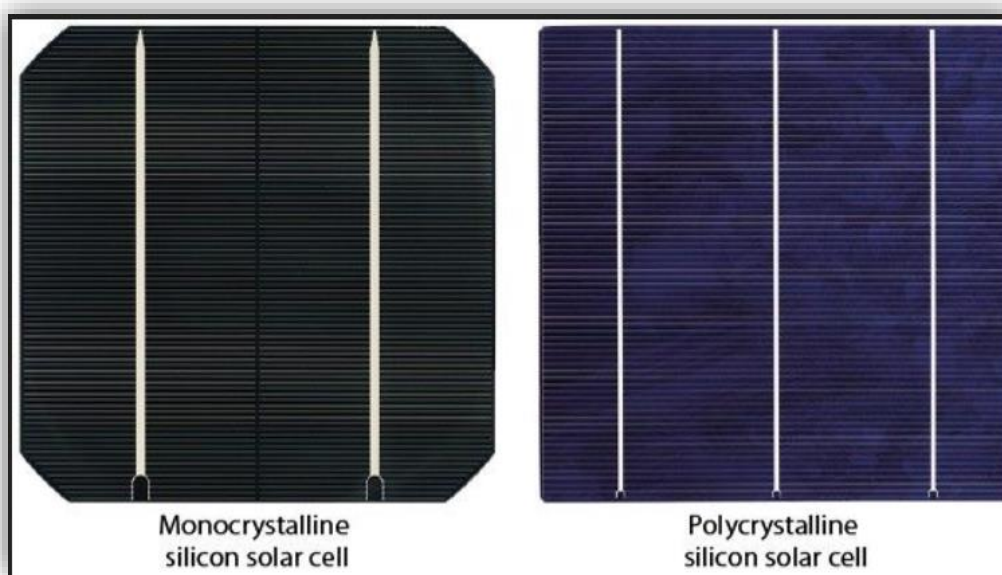
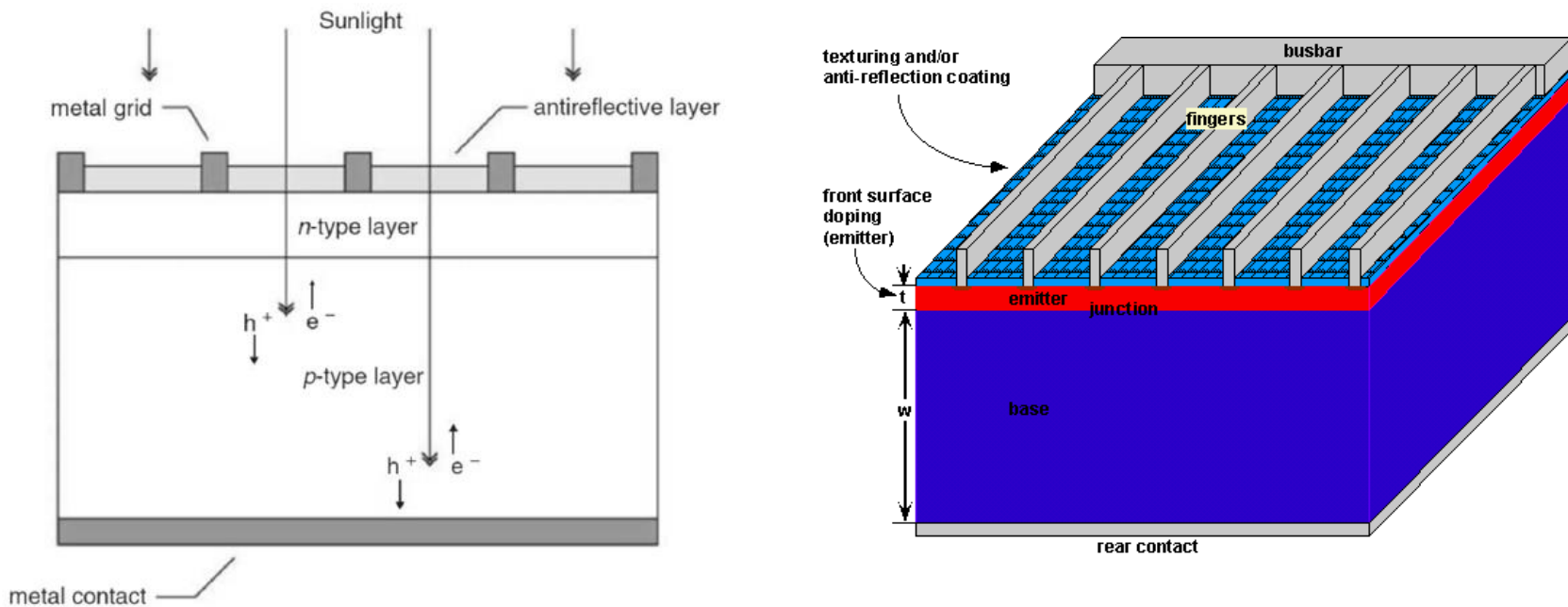


Fig. 7.5. Density of states (*left column*), Fermi distribution (*center column*) and carrier concentration (*right column*) for (a) n-type, (b) intrinsic and (c) p-type semiconductors in thermal equilibrium

Si Solar Cell

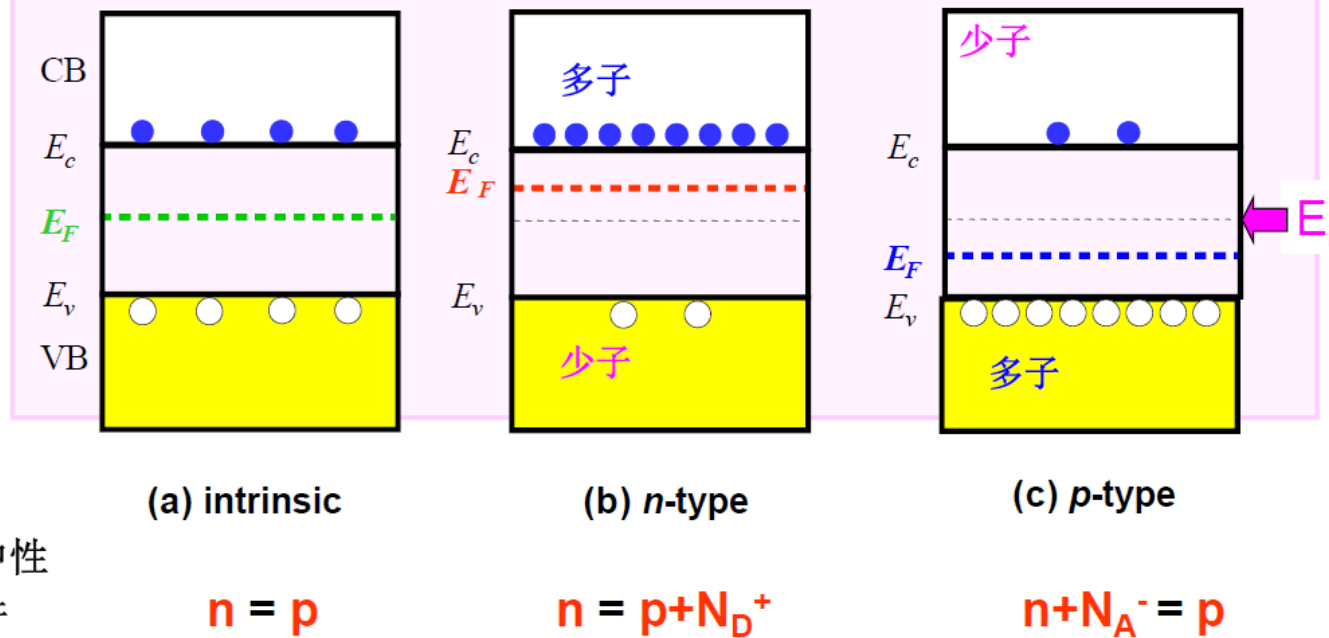


费米能级的高低是电子填充水平的标志。

质量作用定律 $np = n_i^2$

$$n = n_i e^{(E_F - E_i)/k_B T}$$

$$p = n_i e^{(E_i - E_F)/k_B T}$$



课堂例题

现有三块半导体Si材料，已知室温下（300K）它们的空穴浓度分别为：

$$p_{01} = 2.25 \times 10^{16} \text{ cm}^{-3}, \quad p_{02} = 1.5 \times 10^{10} \text{ cm}^{-3}, \quad p_{03} = 2.25 \times 10^4 \text{ cm}^{-3}.$$

- (1) 分别计算这三块材料的电子浓度；
- (2) 判断这三块材料的导电类型；
- (3) 分别计算这三块材料的费米能级的位置。

解答：(1)和(2) 室温时Si的 $E_g = 1.12 \text{ eV}$, $n_i = 1.5 \times 10^{10} \text{ cm}^{-3}$

浓度积 $np = n_i^2$

$$n = \frac{n_i^2}{p} \left\{ \begin{array}{l} n_{01} = \frac{n_i^2}{p_{01}} = 1 \times 10^4 \text{ cm}^{-3} [< p_{01}, \text{ } p\text{-型半导体}] \\ n_{02} = \frac{n_i^2}{p_{02}} = 1.5 \times 10^{10} \text{ cm}^{-3} [= p_{02} = n_i, \text{ } \text{本征半导体}] \\ n_{03} = \frac{n_i^2}{p_{03}} = 1 \times 10^{16} \text{ cm}^{-3} [> p_{03}, \text{ } n\text{-型半导体}] \end{array} \right.$$

(3). 当 $T=300\text{K}$ 时, $k_B T=0.026\text{eV}$

$$p = n_i e^{\frac{E_i - E_F}{k_B T}} \quad E_i - E_F = (k_B T) \ln \frac{p}{n_i}$$

$$p_{01} = 2.25 \times 10^{16} \text{cm}^{-3}$$

$$E_i - E_F = 0.026 \ln \frac{2.25 \times 10^{16}}{1.5 \times 10^{10}} = 0.37\text{eV}$$

P型半导体, Fermi能级在本征Fermi能级以下0.37eV处。

$$p_{02} = 1.5 \times 10^{10} \text{cm}^{-3}$$

$$E_i - E_F = 0.026 \ln \frac{1.5 \times 10^{16}}{1.5 \times 10^{10}} = 0\text{eV}$$

本征半导体, Fermi能级位于本征Fermi能级。

$$p_{03} = 2.25 \times 10^4 \text{cm}^{-3}$$

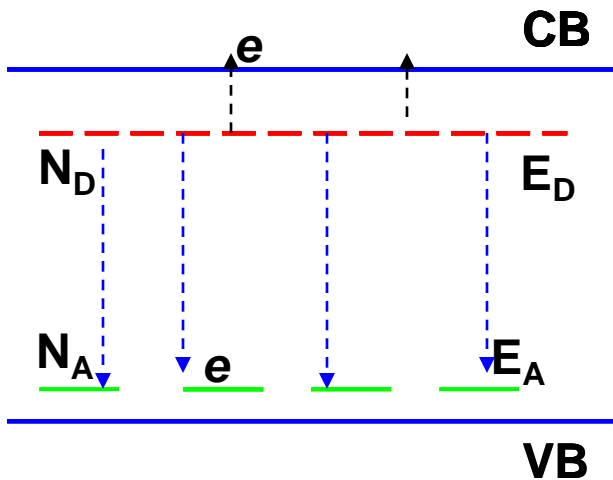
$$E_i - E_F = 0.026 \ln \frac{2.25 \times 10^4}{1.5 \times 10^{10}} = -0.35\text{eV}$$

n型半导体, Fermi能级在本征Fermi能级以上0.35eV处。

有关半导体掺杂的几个补充概念

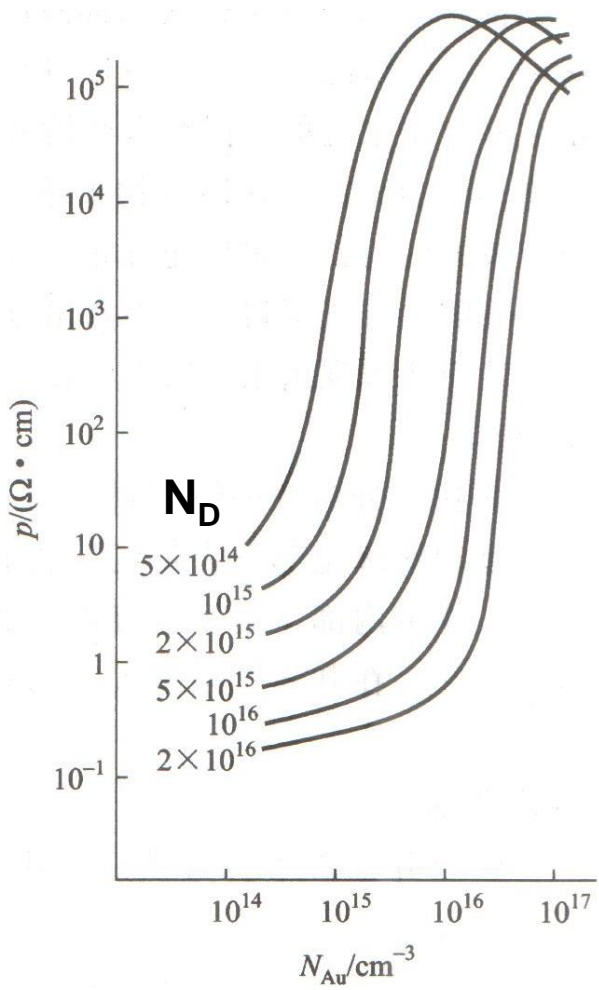
• 补偿

- 施主和受主之间的相互抵消作用。
- 施主电离时，将首先填充受主能级，称之为补偿。
- 最多只能提供 $N_D - N_A$ 个电子。

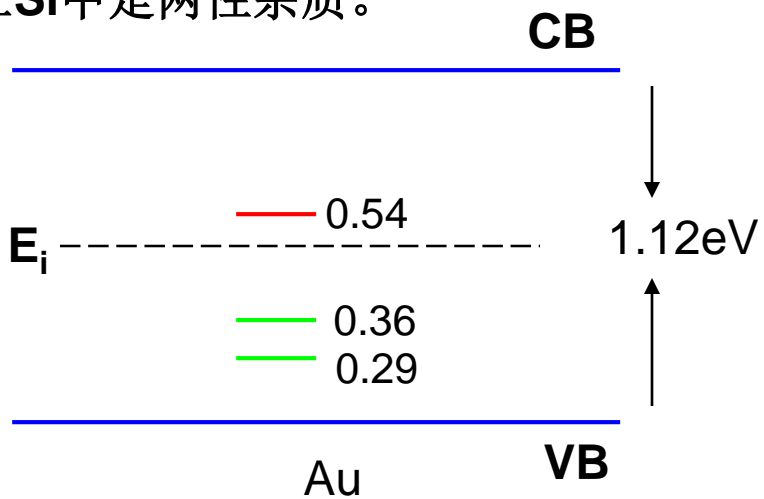


$$E_F = E_D + k_B T \ln \frac{N_D - N_A}{g_D N_A}$$

• 补偿性半绝缘的半导体



- 金在Si中是两性杂质。

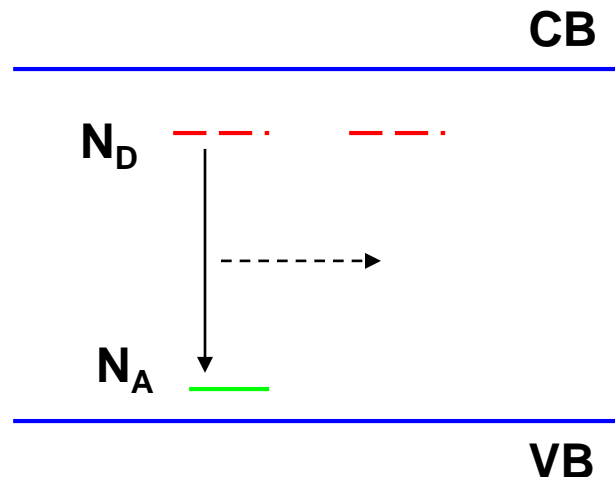


- $N_{\text{Au}} < N_D$: 正常情况;
- $N_{\text{Au}} > N_D$: 浅施主上的电子全部转移到金受主，从而将费米能级钳制在金受主附近;
- Si表现出n型、高阻。

• 宽禁带半导体的掺杂和自补偿

- **双极性半导体**: 可以通过掺杂比较容易获得n/p型导电的半导体;
- 但一些宽带隙半导体 (II-IV; III-V) 常常只容易获得一种导电类型的半导体
- **自补偿**: 半导体中的某种本征缺陷对一种类型的杂质 (受主或施主), 具有自发的补偿效应。

例如: p-ZnO的掺杂困境



- **Donor**: 形成能级为 H^A , 较小, 高温生长过程中, 自由移动, 达到平衡。
- 掺入 **Acceptor** 以后, 将会发生自补偿现象,
- 释放出能量: $E_g - (E_D + E_A) > H^A$, 导致更多的 **Donor** 产生, 难以实现 p型掺杂。

- 半导体掺杂困难的其它因素

- 高的电离能（掺入的是深能级杂质）
- 掺杂剂的溶解度过小
- 施主形成DX中心，引起自补偿 ($2D^0 \rightarrow D^+ + DX^-$)
- 杂质占据不同的晶格位分布引起**donor**和**acceptor**作用
- H的钝化作用（负U性质的两性杂质）

在半导体中实现高浓度掺杂是可能的，
也是很重要的。

3.6 简并半导体

一、产生简并的原因

- 处于饱和电离区的n型掺杂半导体的费米能级位置：

$$E_F = E_C + k_B T \ln \left[\frac{N_D}{N_C} \right]$$

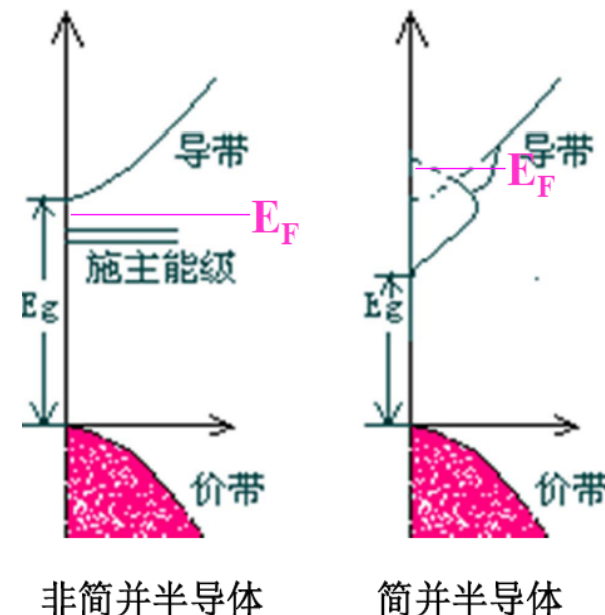
- 当掺杂浓度增大： $N_D \geq N_C$ 时， E_F 将于 E_C 重合，或 $E_F > E_C$ ，即 E_F 进入导带。
- 简并化条件

- | | |
|------------------------------|-----|
| (1) $E_C - E_F > 2k_B T$ | 非简并 |
| (2) $0 < E_C - E_F < 2k_B T$ | 弱简并 |
| (3) $E_C - E_F \leq 0$ | 简 并 |

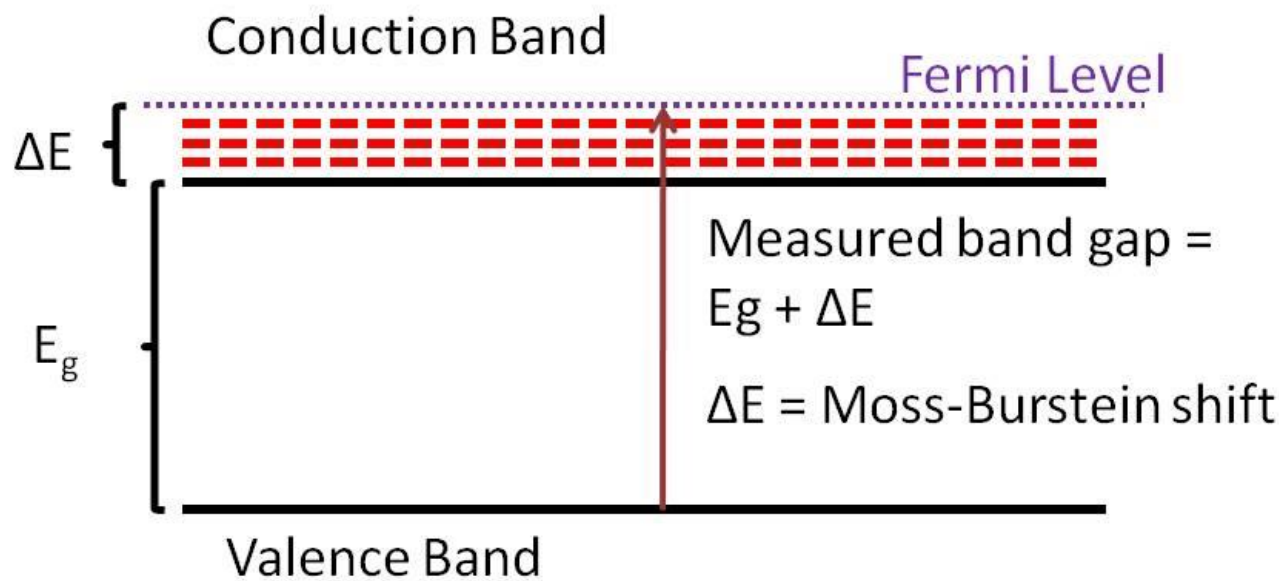
n型半导体的简并条件： $E_F - E_C \geq 0$

p型半导体的简并条件： $E_V - E_F \geq 0$

Fermi能级进入导带或者价带



➤ 重掺杂导致的半导体能带变化（1）：Burstein-Moss效应



- The **Burstein–Moss effect** is the process by which the **apparent bandgap of a semiconductor** (光谱测量结果) is increased as the absorption edge is pushed to **higher energies** as a result of all states close to the conduction band being populated.
- This is observed for a degenerate electron distribution such as that found in some **Degenerate semiconductors** and is known as a **Burstein–Moss shift**.

Anomalous Optical Absorption Limit in InSb

ELIAS BURSTEIN

Crystal Branch, Metallurgy Division, Naval Research Laboratory,
Washington, D. C.

(Received December 11, 1953)

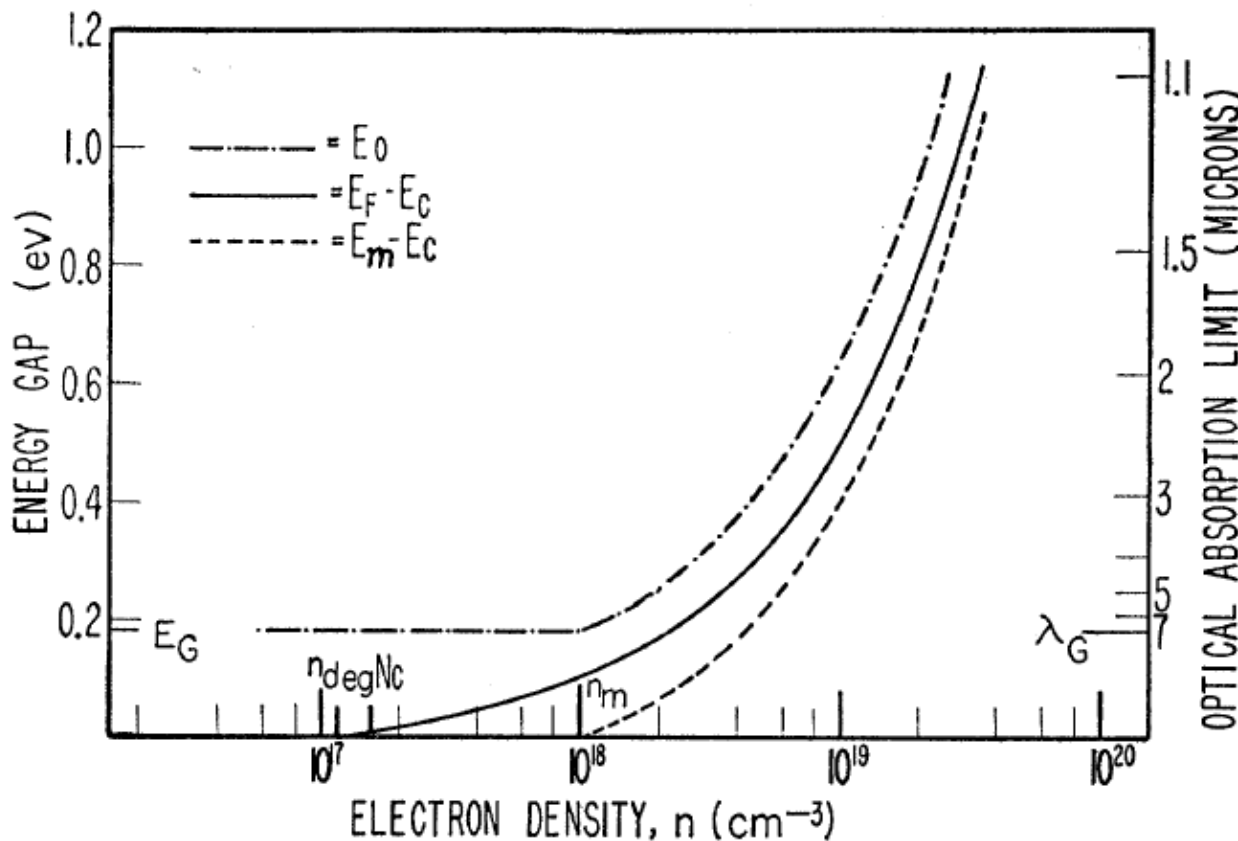


FIG. 2. The dependence of the Fermi level, the lowest unfilled level in the conduction band, and the optical energy gap on charge carrier density in n -type InSb.

➤ 重掺杂导致的半导体能带变化（2）：

Band Gap Renormalization (BGR) effect

- The band structure theory has been developed so far for small carrier densities.
- If the carrier density is large the interaction of free carriers has to be considered. The first step was exciton formation. However, at high temperatures (ionization) and at large carrier density (screening) the exciton is not stable.
- Exchange and correlation energy leads to a **decrease** of the optical absorption edge that is called **band gap renormalization (BGR)**.

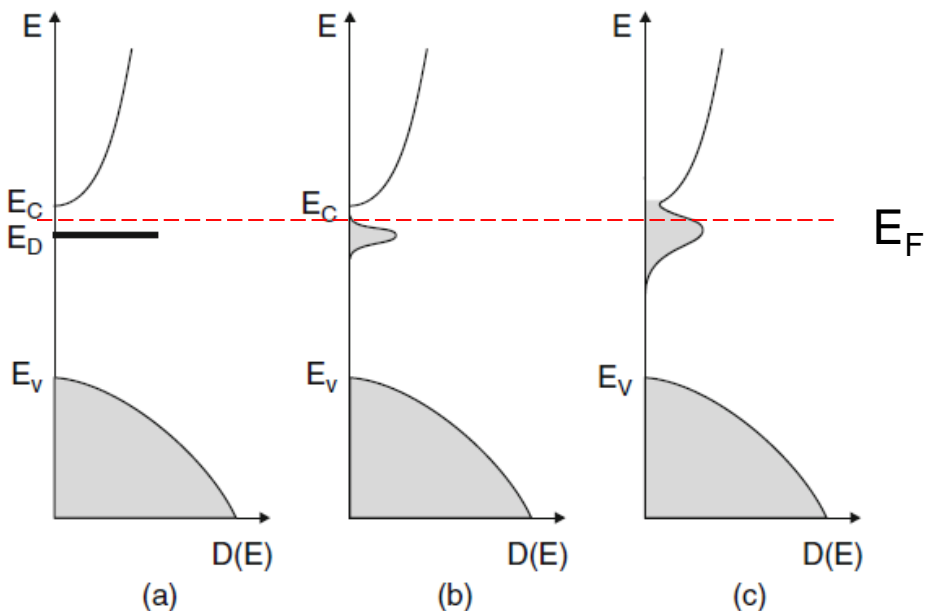


Fig. 7.24. Principle of the formation of a (donor) impurity band. (a) Small doping concentration and sharply defined impurity state at E_D , (b) increasing doping and development of an impurity band that (c) widens further and eventually overlaps with the conduction band for high impurity concentration. The *shaded areas* indicate populated states at $T = 0\text{ K}$

- With increasing concentration, an impurity band develops.
- A periodic arrangement of impurity atoms would result in well defined band edges as found in the Kronig–Penney model.
- Since the impurity atoms are randomly distributed, the band edges exhibit tails.
- For high doping, the impurity band overlaps with the conduction band.

由能带重整化引起的带隙减少了量 (ΔE_{BGR}) 的估算

It has been proposed that these many-body interactions give rise to the band-gap shrinkage ΔE_g^{BN} , which is evaluated for n-ZnO as^{19,20}

$$\begin{aligned}\Delta E_{BGR} = & K_1 n_e^{1/3} + K_2 \left(\frac{m_c^*}{m_e} \right)^{1/4} n_e^{1/4} \\ & + K_3 \left(\frac{m_e}{m_c^*} \right)^{1/2} \left(1 + \frac{m_h^*}{m_c^*} \right) n_e^{1/2},\end{aligned}\quad (7)$$

where each term accounts for the electron exchange interactions, minority-carrier correlations, and carrier-ion correlations.

¹⁹S. C. Jain, J. M. McGregor, and D. J. Roulston, *J. Appl. Phys.* **68**, 3749 (1990).

²⁰J. A. Sans, J. F. Sánchez-Royo, A. Segura, G. Tobias, and E. Canadell, *Phys. Rev. B* **79**, 195105 (2009).

Band-gap tailoring of ZnO by means of heavy Al doping

B. E. Sernelius*

Solid State Division, Oak Ridge National Laboratory, Oak Ridge, Tennessee 37831 (1983)

and Department of Physics, University of Tennessee, Knoxville, Tennessee 37996

$$\Delta E_g = \Delta E_{BM} - \Delta E_{BGR}$$

e.g.

$$\Delta E_g = A n^{1/3}$$

$$\Delta E_3^{\text{BGN}} = P \left(\frac{n_e - n_c}{n_c} \right)^\gamma$$

$$\Delta E^{\text{BGN}} = A n_e^{1/3} + B n_e^{1/4} + C n_e^{1/2}$$

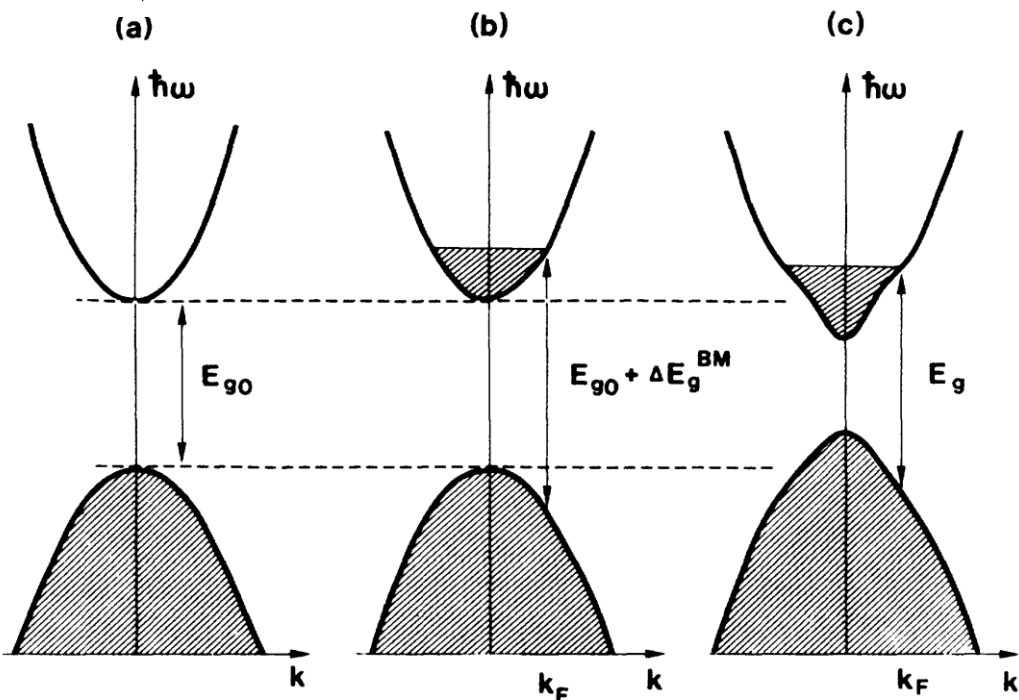


FIG. 3. Schematic band structure with parabolic conduction and valence bands separated by E_{g0} [part (a)], after heavy doping assumed to have the sole effect of blocking the lowest states in the conduction band so that the optical gap is widened by a Burstein-Moss shift ΔE_g^{BM} [part (b)], and representation of a perturbed band structure and ensuing optical band gap E_g in the case of many-body interactions [part (c)]. Shaded areas denote occupied states. The Fermi wave vector k_F is indicated.

Carrier concentration dependence of band gap shift in *n*-type ZnO:Al films

J. G. Lu^{a)} and S. Fujita^{b)}

International Innovation Center, Kyoto University, Katsura, Nishikyo-ku, Kyoto 615-8520, Japan

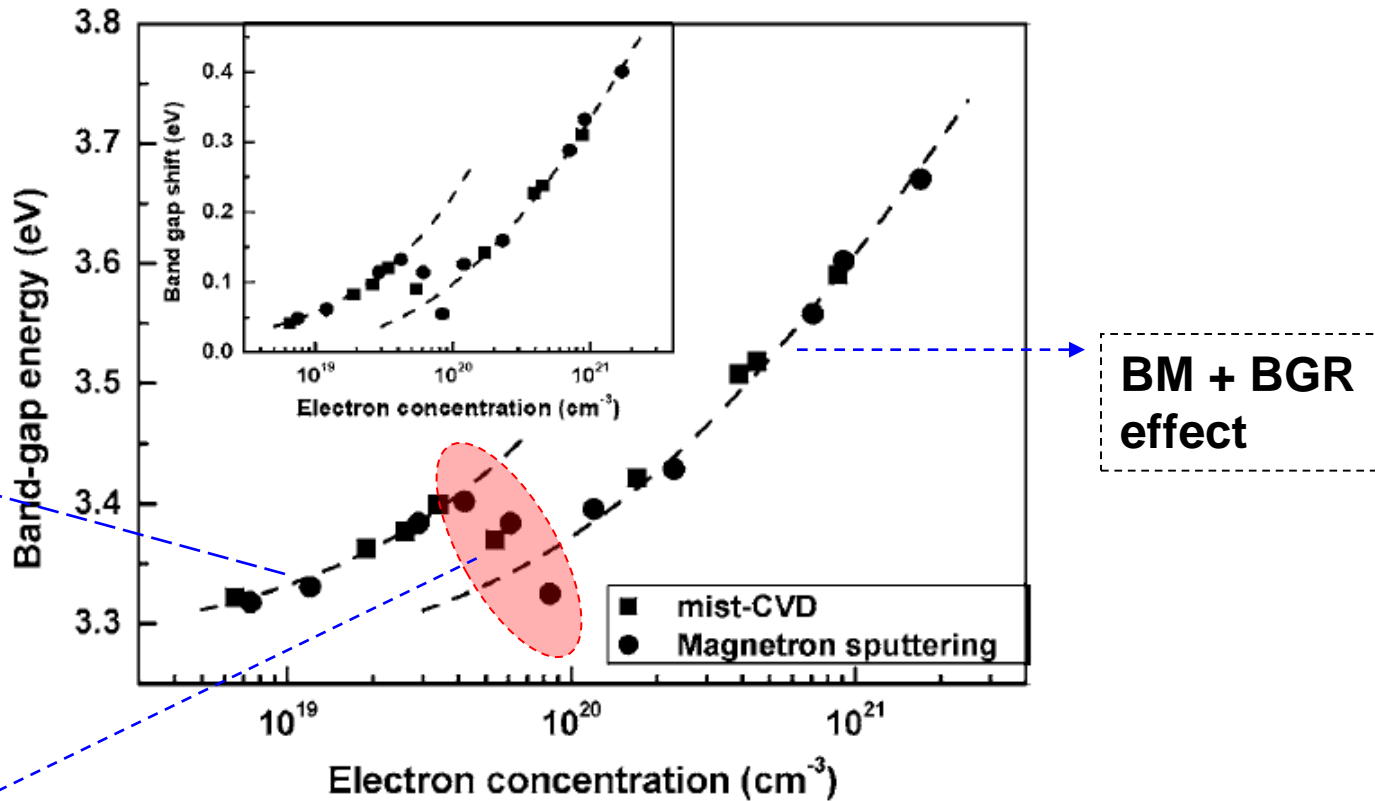


FIG. 4. Band gap energy as a function of electron concentration in AZO. The inset shows the band gap shift as a function of electron concentration. The variation in energy gap is the combined effects of band gap widening caused by BM band filling and band gap narrowing induced by band gap renormalization.

二、半导体产生简并的判据

n型半导体： $N_D \sim N_C$
(杂质浓度判据)

p型半导体： $N_A \sim N_V$

GaAs、Si以及Ge发生简并时所需的杂质浓度：

	N_A (cm^{-3})	N_D (cm^{-3})
Ge	$>10^{18}$	$>10^{18}$
Si	$>10^{18}$	$>10^{18}$
GaAs	$>10^{13}$	$>10^{17}$

➤ Mott Criterion

When the distance of the impurities becomes comparable to their Bohr radius, the critical density (N_{MC}) can result to degeneration.

$$\frac{3}{2\pi} \left(\frac{1}{N_{MC}} \right)^{1/3} = 2a_B$$

$$(N_{MC} * a_B = 0.25)$$

Critical doping concentration for various semiconductors at room temperature.

material	type	N_{MC} (cm^{-3})	Ref.
C:B	p	2×10^{20}	[399]
Ge:As	n	1.5×10^{17}	[421]
Si:P	n	1.3×10^{18}	[423]
Si:B	p	6.2×10^{18}	[423]
GaAs	n	1.0×10^{16}	[424]
GaP:Si	n	6×10^{19}	[426]
GaP:Zn	p	2×10^{19}	[427]
GaN:Si	n	2×10^{18}	[428]
GaN:Mg	p	4×10^{20}	[403]
Al _{0.23} Ga _{0.77} N:Si	n	3.5×10^{18}	[429]
ZnTe:Li	p	4×10^{18}	[422]
ZnTe:P	p	6×10^{18}	[422]
ZnO:Al	n	8×10^{18}	[430]

三、简并半导体中的载流子浓度

- 计算方法同非简并半导体
- 把Boltzmann分布改为Fermi分布

用费米分布函数计算,于是简并半导体的电子浓度 n_0 为

$$n_0 = \frac{4\pi(2m_n^*)^{3/2}}{h^3} \int_{E_c}^{\infty} \frac{(E - E_c)^{1/2} dE}{1 + \exp\left(\frac{E - E_F}{k_0 T}\right)}$$

$$N_e = \frac{2(2\pi m_n^* k_0 T)^{3/2}}{h^3}, x = \frac{E - E_c}{k_0 T}, \xi = \frac{E_F - E_c}{k_0 T}$$

$$n_0 = N_e \frac{2}{\sqrt{\pi}} \int_0^{\infty} \frac{x^{1/2}}{1 + e^{x-\xi}} dx$$

$$\int_0^{\infty} \frac{x^{1/2}}{1 + e^{x-\xi}} dx = F_{1/2}(\xi) = F_{1/2}\left(\frac{E_F - E_c}{k_0 T}\right) \quad (\text{费米积分})$$

- 利用费米积分, 计算发生简并的半导体临界浓度 (刘恩科, p. 84)
- n. p=?

四、简并半导体的杂质离化能与冻析效应

➤ 杂质离化能减小

the binding energy (ionization energy) E_D^b of the electron to the shallow donor is

$$E_D^b = \frac{m_e^*}{m_0} \frac{1}{\epsilon_r^2} \frac{m_0 e^4}{2(4\pi\epsilon_0\hbar)^2}$$

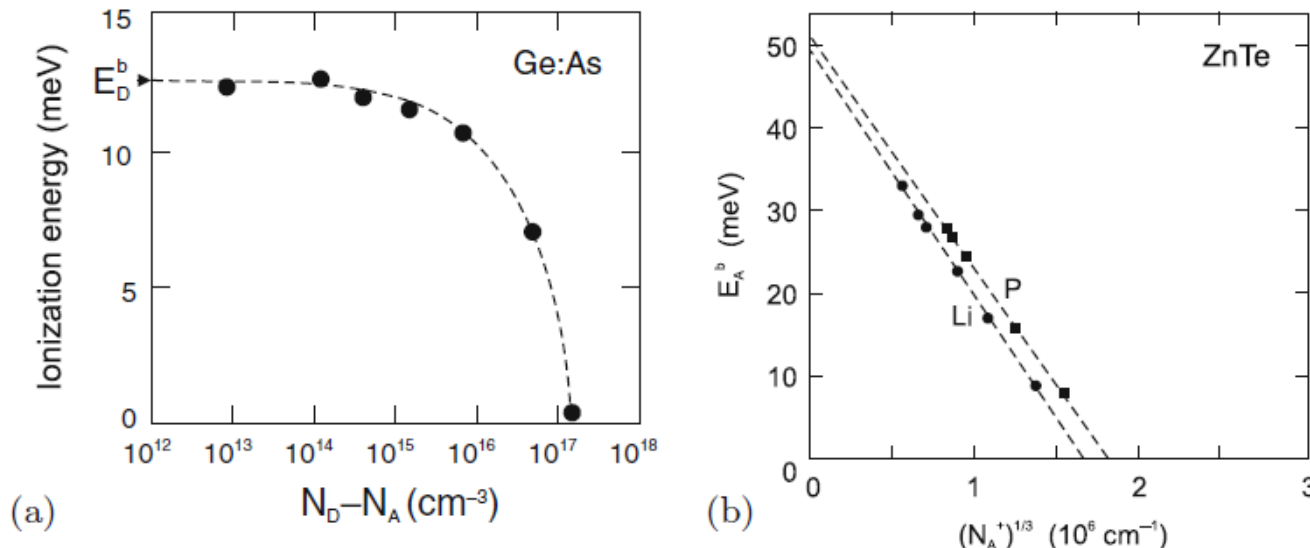
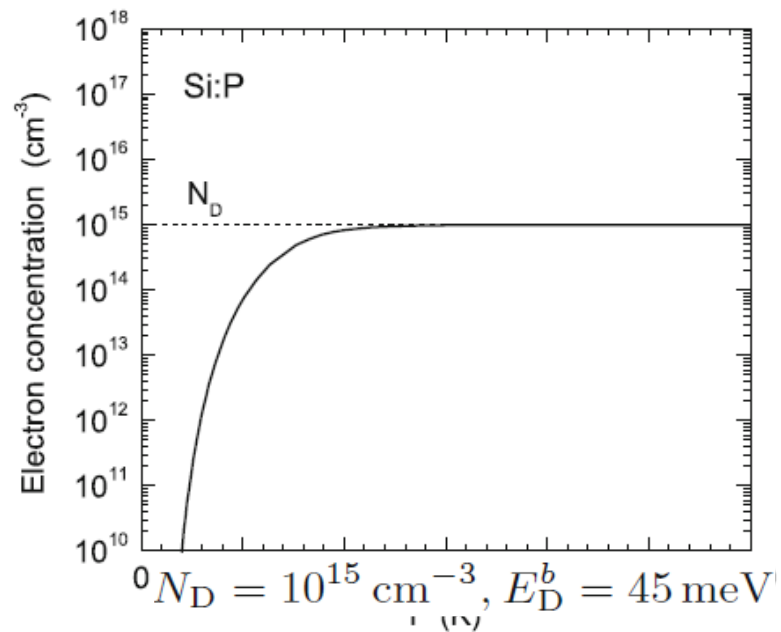
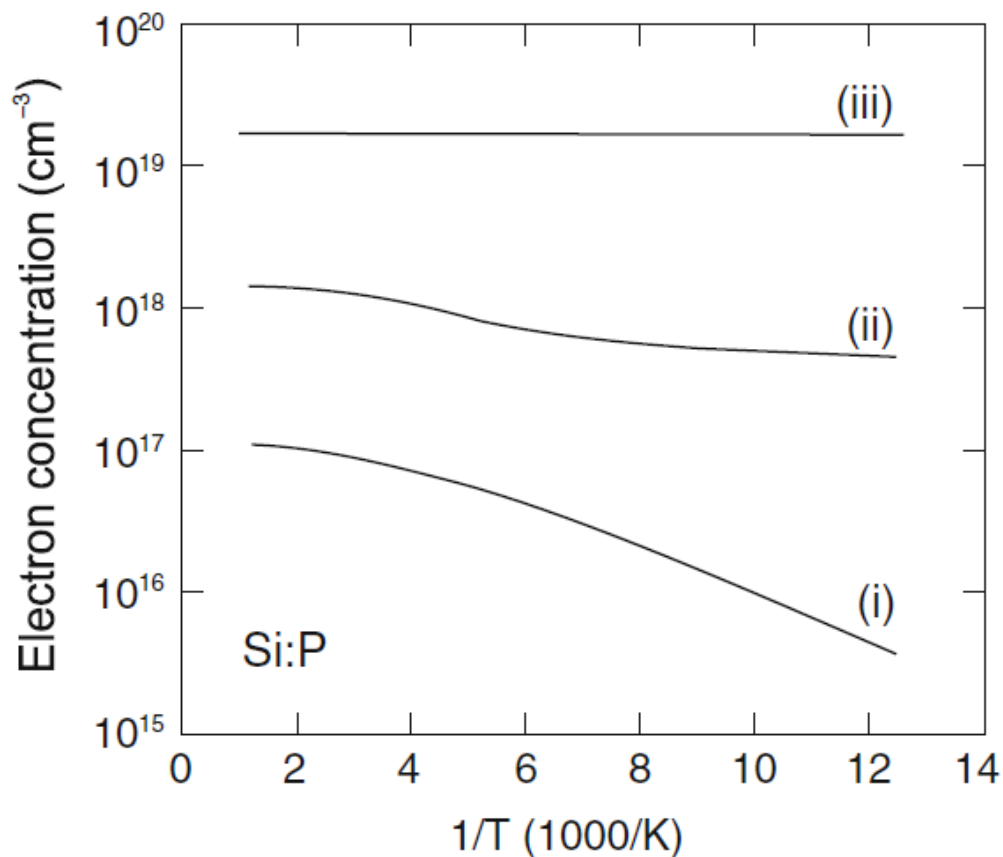


Fig. 7.25. (a) Donor ionization energy in n-type Ge for various doping concentrations. *Dashed line* is a guide to the eye. The arrow labeled E_D^b denotes the low-concentration limit (cf. Table 7.2). Experimental data from [421]. (b) Acceptor ionization energy for ZnTe:Li and ZnTe:P as a function of the third root of the ionized acceptor concentration. Data from [422]

➤载流子冻析效应消失。

The freeze-out of the carrier concentration disappears



(非简并半导体的冻析效应)

Fig. 7.26. Electron concentration vs. inverse temperature for Si:P for three different doping concentrations ((i): $1.2 \times 10^{17} \text{ cm}^{-3}$, (ii): $1.25 \times 10^{18} \text{ cm}^{-3}$, (iii): $1.8 \times 10^{19} \text{ cm}^{-3}$). Experimental data from [423]